Dynamical Chiral Symmetry Breaking in Sliding Nanotubes

X. H. Zhang,[1,2] G. E. Santoro,[1,2,3] U. Tartaglino,[2,1] and E. Tosatti[1,2,3]
[1]*International School for Advanced Studies (SISSA), Via Beirut 2-4, I-34014 Trieste, Italy*
[2]*CNR-INFM Democritos National Simulation Center, Via Beirut 2-4, I-34014 Trieste, Italy*
[3]*International Centre for Theoretical Physics (ICTP), P.O. Box 586, I-34014 Trieste, Italy*
(Received 17 December 2008; published 23 March 2009)

We discover in simulations of sliding coaxial nanotubes an unanticipated example of dynamical symmetry breaking taking place at the nanoscale. While both nanotubes are perfectly left-right symmetric and nonchiral, a nonzero angular momentum of phonon origin appears spontaneously at a series of critical sliding velocities, in correspondence with large peaks of the sliding friction. The nonlinear equations governing this phenomenon resemble the rotational instability of a forced string. However, several new elements, exquisitely "nano" appear here, with the crucial involvement of umklapp and of sliding nanofriction.

DOI: 10.1103/PhysRevLett.102.125502 PACS numbers: 62.25.Jk, 05.45.−a, 47.20.Ky, 63.22.Gh

A popular high-school physics demo is a clamped oscillating rope or guitar string. While being imparted a strictly planar vibration at one end, the string initially vibrates, as expected, within the plane. Above a certain amplitude however the plane of vibration spontaneously and unexpectedly begins to turn around, right or left with equal probability [1]. Since all along the string's Lagrangian (including the external forcing) remains completely left-right symmetric (i.e., nonchiral) this is a prototype example of what may be called dynamical chirality breaking taking place in the macroscopic world. Dynamical spontaneous symmetry breaking of chiral symmetry is actually rife in nature, including examples such as the Taylor-Couette instability in hydrodynamics [2], the spontaneous chirality of vibrating cilia in biology [3] and many other macroscopic scale examples.

We discovered, in simulations of the frictional sliding of carbon nanotubes, a nanoscale example of dynamical chiral symmetry breaking, in particular, in two coaxial nanotubes, one forced to slide inside the other. While both nanotubes are perfectly left-right symmetric and nonchiral, angular momentum strikingly jumps to nonzero values in correspondence to some sliding velocities, coincident with large phonon-related peaks of the sliding friction. The theory of this phenomenon yields nonlinear equations that differ from the string problem by newer elements that are exquisitely nano, now involving umklapp processes and sliding nanofriction.

We conducted classical molecular dynamics simulations of an inner, infinite and termination-free, (5,5) armchair single-wall carbon nanotube sliding at speed v inside a coaxial (10,10) nanotube, as in Fig. 1(a). Standard empirical potentials were used for the intratube [4] and intertube [5] interactions. Details of simulation are given in Ref. [6]. Temperature was controlled, usually at $T = 300$ K, by an algorithm designed to preserve angular momentum [7]. As noted earlier by Tangney *et al.* [8], the tube-tube sliding friction is not hydrodynamical, in fact not even monotonic with v, but develops sharp peaks and onsets at selected speeds. We found sharp frictional peaks near $v = 450$ m/s, 570 m/s, 720 m/s, and an important threshold onset near 780 m/s, shown in Fig. 1(b). These peaks are known to generally arise out of parametric excitation of outer nanotube "breathing" phonon modes, classified by

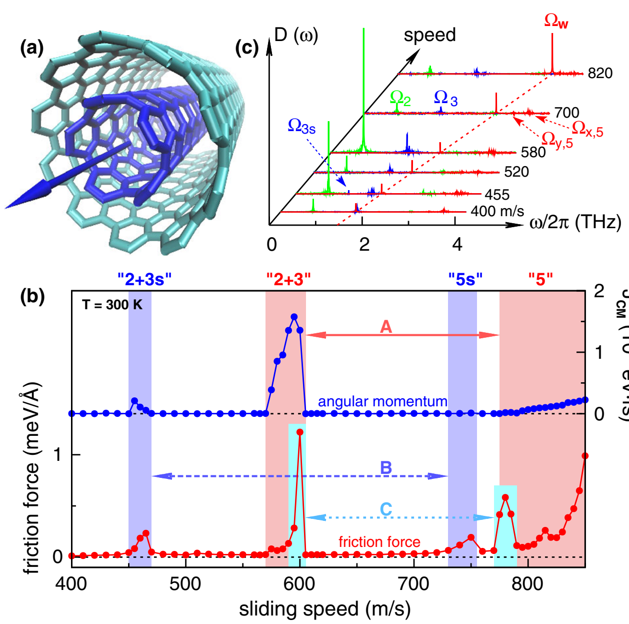

FIG. 1 (color online). (a) Coaxial sliding of (5,5)@(10,10) nanotubes. (b) Sliding friction force per innertube atom and angular momentum J_{CM} from simulations versus speed v at $T = 300$ K. Note the frictional peaks and the threshold near 780 m/s. The nonzero angular momentum signals nanoscale dynamical chiral symmetry breaking in correspondence with the threshold, and with peaks at 570 m/s and 450 m/s. A, B, and C designate related resonance regions, described in text. (c) Outer tube radial motion Fourier spectra with $n = 2$ (green), 3 (blue), and 5 (red) symmetry, showing resonant enhancement in correspondence with peaks and threshold.

an angular momentum index n (for tangential quantization around the tube axis). Our peak positions differ from earlier ones [8] due to our lack of tube terminations (implying mode uniformity along the tube), and also to our different intertube potentials. As noted earlier [6], the nonmonotonic F-v characteristics implies a "negative differential friction", whereby an increasing applied force F yields an inner-tube velocity that grows by jumps and plateaus, rather than smoothly.

The surprise comes from analyzing, at the frictional peaks, the two parts of angular momentum J around the tube axis y: its center-of-mass (rigid body rotation with angular velocity ω) and shape-rotation ("pseudorotational") parts $J = J_{\rm CM} + J_{\rm pseudo}$, with $J_{\rm CM} = \sum_i m_i[\vec{r}_i \times (\vec{\omega} \times \vec{r}_i)]_y$, and $J_{\rm pseudo} = \sum_i m_i(\vec{r}_i \times \dot{\vec{r}}_i)_y$. Generally zero at generic v due to lack of nanotube chirality, $J_{\rm pseudo} = -J_{\rm CM} = 0$, $J_{\rm pseudo}$ jumps to nonzero values at the frictional peaks and past the threshold, where $J_{\rm pseudo} = -J_{\rm CM} \neq 0$ (total J is clearly conserved); see Fig. 1(b). Simulations at lower temperatures (not shown) reveal other smaller frictional peaks, but the main findings of the present Letter, including chirality breaking, are still present, and indeed even stronger.

Cross-section snapshots at intervals of 50 fs, at $v = 820$ m/s of Fig. 2 show a large pentagonal distortion of the outer tube, corresponding to an $n = 5$ breathing mode. A vertex of the pentagon moves clockwise (or counterclockwise with 50–50 probability in different simulations) with angular velocity $\Omega_w/5$, where $\Omega_w = 2\pi v/a$ is the "washboard" frequency associated with the sliding speed v and $a = 2.46$ Å is the intertube potential periodicity. The pentagon rotation signals a nonvanishing $J_{\rm pseudo} > 0$. Since the total $J = 0$, the center-of-mass acquires an equal and opposite counterrotation $J_{\rm CM} = -J_{\rm pseudo} < 0$, as demonstrated by the red atom marker in Fig. 2.

Theory.—The mechanism underlying symmetry breaking is the tube nonlinearity, reminiscent of the string instability [1]. The nonlinear motion of a string forced to vibrate along a transverse direction x at frequency Ω is described by

$$\ddot{X} = -[\omega_{k,T}^2 + K(|X|^2 + |Y|^2)]X + F\cos(\Omega t),$$
$$\ddot{Y} = -[\omega_{k,T}^2 + K(|X|^2 + |Y|^2)]Y, \tag{1}$$

where $\omega_{k,T} = k\sqrt{\mu/M}$ is the bare transverse frequency with wave vector k (μ is the Lamé constant and M the mass density), X, Y are two orthogonal linear polarizations, and F is the forcing amplitude. The nonlinearity $K > 0$ accounts for the increase of the transverse frequency at large amplitudes, where the larger overall elongation leads to an effective string tension increase. Because of $K > 0$ there is a critical frequency $\Omega_{\rm cr} = \sqrt{\omega_{k,T}^2 + (KF^2/16)^{1/3}}$ beyond which the string, although forced along x, spontaneously develops both X and Y modes, an elliptic polarization resulting from a purely linear forcing, with a spontaneous dynamical chirality breaking. The critical amplitude of the X-mode beyond which the elliptical polarization sets in is $(2F/K)^{1/3}$ (this will be demonstrated in Fig. 3(b) below). In the nanotube case, the sliding inner tube excites phonon modes of the outer one, uniformly along the tube in our termination-free case. The outer (10,10) nanotube has, among others, doubly degenerate modes with angular momentum $n = \pm 2$, ± 3, ± 4, and ± 5, etc. Let $u_x(\theta)$ and $u_z(\theta)$ be displacements in the x (tangential) and z (radial) directions at angular position θ on the outer tube circumference, and $u_{n,x,\pm}$ and $u_{n,z,\pm}$ their respective n-mode amplitudes, traveling clockwise (+) and counterclockwise (−). Suzuura and Ando (SA) [9] described these modes at the quadratic level in a continuum model. Third- and fourth-order energy terms in u mix the different n modes in all possible ways compat-

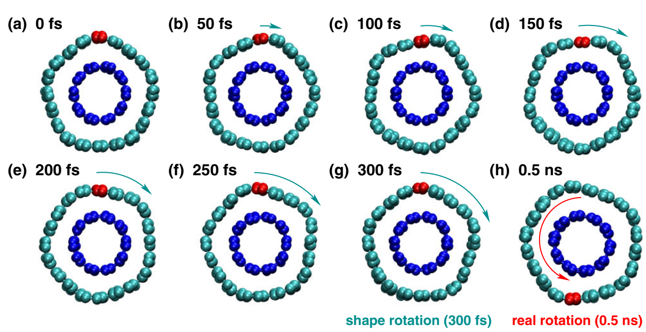

FIG. 2 (color online). Tube cross sections, showing a shape rotation (pseudorotation) and an overall rotation (marked by red atoms) for $v = 820$ m/s (washboard period $a/v = 300$ fs). (a)–(g) Snapshots at intervals of 50 fs comprise one period of pseudorotation, where the pentagon shape rotates clockwise. (h) An overall counterrotation of nearly π in 0.5 ns.

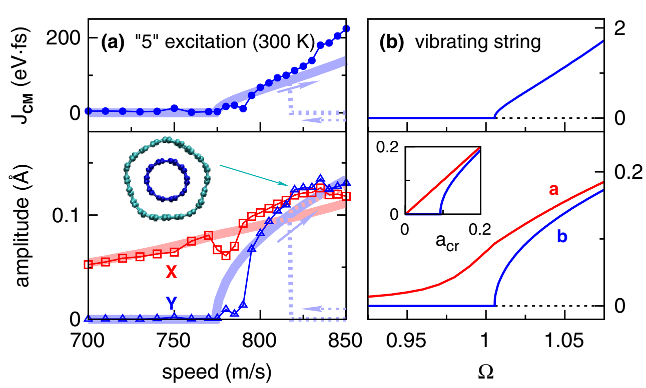

FIG. 3 (color online). (a) Simulation results (dots) in the threshold region $v > 780$ m/s, compared with the model (thick solid and dotted lines) of Eqs. (2). X, $Y = |u_{z,5,+} \pm u^*_{z,5,-}|$ are amplitudes of $X(t)$ and $Y(t)$ defined in the text. Y becomes nonzero together with nonzero $J_{\rm CM} = -J_{\rm pseudo}$ above the critical threshold speed. The hysteresis found in the model is absent in the simulation. (b) Forced vibrating string from Eqs. (1), with $\omega_{k,T} = 1$, $K = 5$, $F = 0.002$, and $M = 100$. a, b are the X, Y-mode amplitudes. The critical frequency $\Omega_{\rm cr} = 1.0054$ and the threshold X-mode amplitude $a_{\rm cr} = 0.093$ (inset).

ible with conservation of angular momentum. The main nonlinear terms $\propto\int dx(\frac{\partial u_x}{\partial x}+\frac{u_z}{R})(\frac{\partial u_z}{\partial x}-\frac{u_x}{R})^2$ to third order, and $\propto\int dx(\frac{\partial u_z}{\partial x}-\frac{u_x}{R})^4$ to fourth order turn out to be as crucial as in the string.

"$n = 5$" *excitation.*—The 10-chain atomic structure of the sliding (5,5) inner tube stimulates at all speeds v the outer tube with a deformation corresponding to a linearly polarized, $k_y = 0$, $n = 5$ mode with a washboard frequency $\Omega_w = 2\pi v/a$. Away from resonance, $\Omega_w < \omega_5$, the excitation amplitude of the $n = 5$ outer tube mode is small, and linear. Near and above resonance, however, the amplitude grows, and nonlinearities become dominant. Starting from the SA model [9] including nonlinearities, after some approximations (mainly $u_{x,n,\pm} \approx (i/n)u_{z,n,\pm}$ as appropriate from linear eigenvector analysis, neglecting small mode-mixing third-order terms while keeping large fourth-order contributions which generate terms such as $|u_{z,5,+/-}|^2 u_{z,5,+}$), we arrive at equations for the $n = \pm 5$ phonon amplitudes of the suggestive form

$$\ddot{X} = -[\omega_5^2 + Q + (P/4)(|X|^2 + |Y|^2)]X + 4F\cos(\Omega_w t),$$
$$\ddot{Y} = -[\omega_5^2 - Q + (P/4)(|X|^2 + |Y|^2)]Y, \quad (2)$$

where the two variables $X(t) = (u_{z,5,+} + u^*_{z,5,-})e^{i\Omega_w t}$ + c.c. and $Y(t) = i(u_{z,5,+} - u^*_{z,5,-})e^{i\Omega_w t}$ + c.c. parameterize the radial displacement $u_{z,5}(\theta, t)$ in terms of two orthogonal standing waves, $u_{z,5}(\theta, t) = X(t)\cos(5\theta) + Y(t)\times\sin(5\theta)$, and the fourth-order term P again shifts upwards the frequency as the amplitude increases. The important difference between Eqs. (2) and those of the string is the "nano" Q term, representing an *umklapp* process coupling two outer tube modes with $n = \pm 5$ through a "reciprocal lattice vector" of the inner tube, with its 10 carbon double chains. The umklapp term splits the X/Y frequencies to approximately $\sqrt{\omega_5^2 \pm Q}$. A static double-tube phonon calculation confirms split frequencies $\omega_x = 3.35$ and $\omega_y = 3.15$ THz which measure the umklapp strength.

In nanotube sliding, unlike a guitar string that can be pinched soft or hard, the only controllable parameter is the speed v. Nevertheless, due to the similar fourth-order nonlinear effects, the physics of nanotube sliding, in the region with $v > 780$ m/s [shaded and labeled "5" in Fig. 1(b)], resembles that of the string, see Fig. 3(a). Near the 780 m/s threshold, $\Omega_w \approx 3.17$ THz, just above $\omega_y = 3.15$ THz, a spontaneous symmetry breaking occurs, the Y amplitude growing from zero, and the center-of-mass angular momentum with it. In the approximations considered so far, this should correspond to a pure "$n = 5$" excitation, and indeed this is close to reality, as shown in the Fourier spectrum of Fig. 1(c), where at $v = 820$ m/s the most important peak appears at the washboard frequency Ω_w. Note that the effective $n = 5$ mode frequency is dragged along by the washboard, growing with v and with the friction magnitude. When the speed grows larger than 830 m/s, simulations show the additional excitation of $n = 2$ or $n = 3$ modes, due to third-order nonlinearites not accounted for in Eqs. (2). Here the dynamics, still chiral, becomes more complex than that of the pure $n = 5$ mode. In Fig. 3(a) solutions of Eqs. (2) are shown as shaded thick lines, with parameters $P = (41\,472/50)\alpha/MR^4$, Q, and F which were fit to the bulk modulus of the nanotube ($\alpha = 15\,000$ Å^2/ps^2), the intrinsic phonon frequencies and the splitting for $n = 5$ ($Q = 50.5/\text{ps}^2$), as well as the energy corrugation ($F = 5$ Å^2/ps^2) of the intertube potential. The model agrees fairly well with hard simulation results, including a crossing of X and Y amplitudes at around $v = 815$ m/s, which only occurs due to umklapp. A feature predicted by the model is a hysteretic behavior with respect to increasing and decreasing v. The hysteresis is not seen in simulations both at 300 and at 50 K. We suspect that frictional Joule heating could be sufficient to remove it. Also, our model being mean-field in character, it does not allow for fluctuations. The simulations of course do, and indeed occasional reversals of the sign of J_{CM} are observed when $|J_{\text{CM}}|$ is very small; these reversals are suppressed, most likely by inertia, when $|J_{\text{CM}}|$ is large.

"$2 + 3 = 5$" *excitation.*—Consider now the main frictional peak labeled "2 + 3" in Fig. 1(b), around $v \approx 570$ m/s. This corresponds, as shown by Fig. 4, to a mixed resonance involving three modes, $n = 2$, 3, and 5 simultaneously [see Fourier spectrum in Fig. 1(c)]. The inset in Fig. 4 shows that the cross-section snapshot of both tubes in this region of v, where frictional excitation is huge, is mostly elliptical, indicating a dominant $n = 2$ deformation [see also the large $n = 2$ peak in the Fourier spectrum of Fig. 1(c)], with a slight triangular ($n = 3$) deformation. Our anharmonic continuum model nicely explains these results, the umklapp terms (present in nanotubes but not in

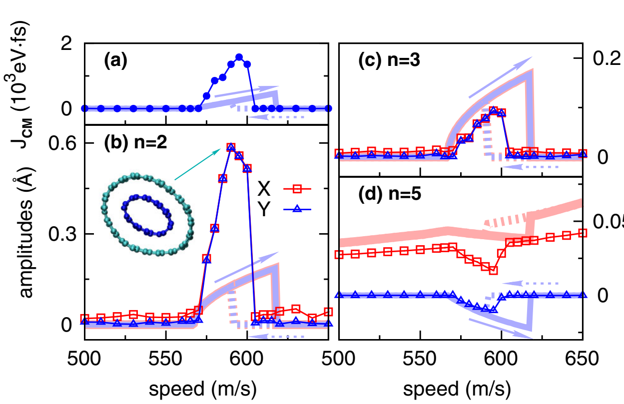

FIG. 4 (color online). Simulation results (dots) and comparison with the model (with a velocity backshift of 78 m/s) for the 2 + 3 peak (thick solid and dotted lines). The model results are based on the 6 equations, generalization of Eqs. (3), for $u_{x,n}$ and $u_{z,n}$ with $n = 2$, 3 and 5. $X_n, Y_n = |u_{z,n,+} \pm u^*_{z,n,-}|$ are amplitudes of $X_n(t)$ and $Y_n(t)$. Y_n becomes nonzero together with nonzero J_{pseudo} above the critical sliding speed, for "2 + 3" excitations. Hysteresis is not seen in the simulation.

the string) playing a crucial role [10]. In this region of v we can truncate the full hierarchy of coupled equations to 6 equations involving the relevant Fourier modes $u_{x/z,n}$ with $n = 2, 3, 5$ [10]. To give a flavor of the full theory [10], we report here the equation of motion for mode $u_{z,5}$, obtained under the linear approximation $u_{x,5} \approx (i/5)u_{z,5}$ [10],

$$\ddot{u}_{z,5} = -\gamma\dot{u}_{z,5} - Qu^*_{z,5} - \left(\omega_5^2 + \sum_{m=2,3,5} B_m|u_{z,m}|^2\right)u_{z,5} - A^{\rm dir}u_{z,2}u_{z,3} + A^{\rm umkl}u^*_{z,2}u^*_{z,3} + 2F\cos(\Omega_w t), \quad (3)$$

where the last term represents the washboard forcing (due to innertube sliding), while the Q term is the previously discussed umklapp term $-5 \rightarrow 5$. (Similar equations hold for the modes $n = 2$, 3, except that the Q term and the explicit forcing are missing.) The physics of the B_m terms is an effective increase of the bare frequency ω_5 due to the excitation of modes $m = 2$, 3, 5, via fourth-order nonlinearities. $A^{\rm dir}$ and $A^{\rm umkl}$ represent the effect of third-order nonlinearities, whereby a combined excitation of modes 2 and 3 can lead, by angular momentum conservation, to a term influencing mode 5 either in a direct way, via $2 + 3 = 5$, or through umklapp, via $-2 - 3 = -5 \rightarrow 5$. The stationary solutions of the nonlinear coupled equations for $u_{x/z,n=2,3,5}$, obtained numerically, reveal a rather simple structure, namely, $u_{x/z,5}(t) = u_{x/z,5,+}e^{i\Omega_w t} + u_{x/z,5,-}e^{-i\Omega_w t}$, $u_{x/z,2}(t) = u_{x/z,2,+}e^{i\Omega_2 t}$, and $u_{x/z,3}(t) = u_{x/z,3,+}e^{i\Omega_3 t}$, with $\Omega_2 + \Omega_3 = \Omega_w$: in words, mode 5 oscillates with the driving washboard frequency Ω_w, while modes 2 and 3 "feel" an indirect driving from mode 5 and oscillate at frequencies Ω_2 and Ω_3 (renormalized by tube-tube coupling and anharmonicity) in such a way as to realize a perfect "resonance" with the driving frequency [see Fourier spectra Fig. 1(c)].

As simulations show, the amplitudes of $X_n = u_{z,n,+} + u^*_{z,n,-}$ and $Y_n = u_{z,n,+} - u^*_{z,n,-}$ (in qualitative agreement between model and simulation) are equal to each other for both $n = 2$ and $n = 3$, implying $u_{z,2/3,-} = 0$. That means, in full agreement with the model, a full chirality for both modes, with waves traveling totally clockwise (or counterclockwise, with equal probability). The $n = 5$ X and Y amplitudes are, on the contrary, unequal and much smaller than $n = 2$ and 3. The continuum model actually predicts—in striking agreement with the simulation—that the $n = 5$ mode rotates opposite to the chirality of modes 2 and 3 (i.e., counterclockwise, $|u_{z,5,-}| > |u_{z,5,+}|$, for the case shown here), an effect entirely due to *umklapp* terms [10].

So far we have explained the two main features labeled A in Fig. 1(b). The features labeled B appear to represent a replica, where single outer tube $n = 3$, 5 excitations replace the double tube ones $n = 3$, 5. For example, in the spectrum for 455 m/s [Fig. 1(c)], the $n = 3s$ mode is at 1.14 THz, the outer tube value, different from the joint $n = 3$ mode where both tubes vibrate together. Analogously, the $n = 5s$ mode is excited at 720 m/s. Here, however, the friction is so small that the excited angular momentum is essentially invisible. The two regions labeled C, finally, are irrelevant to the present context and will be discussed elsewhere [10].

In summary we have described a spontaneous breaking of chiral symmetry occurring in nanoscale friction. Our very large speeds and termination-free conditions differ strongly from experimental conditions where nanotube sliding was observed so far [11]. Attempts at observing this chirality breaking could nonetheless be of considerable interest, considering in addition the possibility to examine the effect of electronic frictional dragging [12] an avenue which seems worth considering. Although the modes that play a major role in electron-phonon coupling [13], and nanotube superconductivity [14] are different, breathing modes excitation was recently demonstrated by STM tips [15]. The physical understanding obtained for our microscopic nonlinear dynamical system might also serve as a prototype for phenomena in the field of nanomotors. Examples of spontaneous chiral symmetry breaking that are relevant to the dynamics of nanomotors have been described in rotaxanes [16], where a series of chemical reactions can give rise to a biased Brownian motion of a small ring around a larger one in either direction. Our example represents a first idealized case where the origin of nanoscale chiral symmetry breaking is strictly physical.

One of the authors (X. H. Z.) thanks Professor X. G. Gong for his encouragement during the research. This research was partially supported by PRIN 2006022847, and by CNR/ESF/EUROCORES/FANAS/AFRI. We thank D. Ceresoli for an illuminating suggestion.

[1] J. A. Elliott, Am. J. Phys. **50**, 1148 (1982).
[2] E. Guyon, J.-P. Hulin, L. Petit, and C. D. Mitescu, *Physical Hydrodynamics* (Oxford University Press, New York, 2001).
[3] P. Lenz *et al.*, Phys. Rev. Lett. **91**, 108104 (2003).
[4] D. W. Brenner, Phys. Rev. B **42**, 9458 (1990).
[5] A. N. Kolmogorov *et al.*, Phys. Rev. B **71**, 235415 (2005).
[6] X.-H. Zhang *et al.*, Surf. Sci. **601**, 3693 (2007).
[7] T. Soddemann *et al.*, Phys. Rev. E **68**, 046702 (2003).
[8] P. Tangney *et al.*, Phys. Rev. Lett. **97**, 195901 (2006).
[9] H. Suzuura *et al.*, Phys. Rev. B **65**, 235412 (2002).
[10] X. H. Zhang *et al.*, (to be published).
[11] J. Cumings *et al.*, Science **289**, 602 (2000).
[12] B. N. J. Persson *et al.*, Phys. Rev. B **69**, 235410 (2004).
[13] S. Piscanec *et al.*, Phys. Rev. B **75**, 035427 (2007).
[14] M. Ferrier *et al.*, Phys. Rev. B **74**, 241402(R) (2006).
[15] B. J. LeRoy *et al.*, Nature (London) **432**, 371 (2004).
[16] J. V. Hernández *et al.*, Science **306**, 1532 (2004).